Prediction of Solubility of α−Olefins in Polyolefins Using a Combined Equation of StateMolecular Dynamics Approach

ARTICLE *in* INDUSTRIAL & ENGINEERING CHEMISTRY RESEARCH · JULY 2006

Impact Factor: 2.59 · DOI: 10.1021/ie060137j

4 AUTHORS, INCLUDING:

Vasileios Kanellopoulos
Borealis
54 PUBLICATIONS **216** CITATIONS
SEE PROFILE

Prokopios Pladis
The Centre for Research and Technology, Hel…
42 PUBLICATIONS **329** CITATIONS
SEE PROFILE

Costas Kiparissides
Aristotle University of Thessaloniki
324 PUBLICATIONS **4,903** CITATIONS
SEE PROFILE

Prediction of Solubility of α-Olefins in Polyolefins Using a Combined Equation of State−Molecular Dynamics Approach

Vassileios Kanellopoulos, Dimitrios Mouratides, Prokopis Pladis, and Costas Kiparissides*

Department of Chemical Engineering and Chemical Process Engineering Research Institute, Aristotle University of Thessaloniki, P.O. Box 472, 54124 Thessaloniki, Greece

In the present study, the Sanchez−Lacombe equation of state (i.e., SL EOS) was employed to calculate the solubilities of α-olefins in polyolefins over a wide range of pressures and temperatures. The characteristic parameters (i.e., P^*, T^*, and ρ^*) of the pure components, appearing in the Sanchez−Lacombe EOS, were estimated using a molecular dynamic procedure (MD). For all binary systems examined, a single binary parameter, k_{ij}, accounting for the interactions between the penetrant molecules and the polymer chains was used to fit model predictions to available solubility measurements. The value of the binary interaction parameter was found to depend on the type of the penetrant molecules, the comonomer type in the ethylene copolymers, and the polymer crystallinity as well as the selected experimental conditions (i.e., temperature and pressure). The theoretically calculated solubilities were found to be in excellent agreement with the corresponding experimentally measured values, demonstrating the capability of the SL EOS to predict the solubility of α-olefins in semicrystalline polyolefins.

Introduction

In the heterogeneous polymerization of olefins, the polymerization rate of the individual catalyst/polymer particles depends on the concentration of catalyst active sites and the monomer solubility in the amorphous polymer phase.[1−3] These variables largely control the reactor productivity as well as the molecular properties of the polyolefin. Thus, knowledge of the solubilities of α-olefins in various polyolefins is of profound importance to the polyolefin industry.

Sorption experiments are commonly employed to determine the solubility of small penetrant molecules in polymers under different conditions (e.g., temperature, pressure, polymer crystallinity, etc.). Existing experimental methods employed to measure the solubility of gases in polymers can be divided into four main classes: (i) gravimetric methods in which the polymer sample's weight is directly measured during a sorption experiment; (ii) oscillating methods in which the increase in mass is deduced from the resonance characteristics of a vibrating support; (iii) pressure decay methods in which the amount of the sorbed species is evaluated from pressure−volume−temperature (PVT) measurements; and (iv) flow measurement methods such as inverse gas chromatography.

In gravimetric methods, the sorption of a single component or of a mixture of components is carried out by exposing a preweighed polymer sample to well controlled experimental conditions and continuously monitoring its weight until equilibrium has been achieved. On the basis of the measured sorption kinetics, the penetrant(s) solubility can be calculated. In oscillatory techniques, the resonant characteristics of a piezoelectric crystal or of a metal reed on which a polymer sample has been placed are monitored in terms of the mass of the sorbed species. Knowledge of the density and viscosity of the gas is required in order to analyze the response of the vibrating sensor. The principle of the pressure decay method is based on the continuous measurement of pressure decrease in a constant volume vessel containing the polymer sample and a known amount of gas. Finally, in flow measurement methods (i.e., inverse gas chromatography), the gas solubility in a polymer is deduced from the measurement of penetrant partitioning between the mobile gas phase and the stationary polymer one.

To predict the equilibrium concentration of a sorbed species in an amorphous polymer phase, an equation of state can be employed. Chen[4] applied the Heuer−Schotte equation of state to calculate the solubility of hydrocarbon vapors in amorphous polyethylene. Sarti and Doghieri[5] presented a predictive model based on the lattice fluid theory to calculate the solubilities of CO_2, N_2, CH_4, and C_2H_4 in polystyrene and polycarbonate. In another publication, Doghieri and Sarti[6] used the NELF (i.e., nonequilibrium lattice fluid) model to calculate the solubility of gases in glassy polymers. Yoon et al.[7] reported that the solubilities of 1-butene, 1-hexene, and 1-octene in linear low density polyethylenes (LLDPEs) could be satisfactory represented by the Flory−Huggins's equation over a wide range of temperatures and concentrations of sorbed species, using a single value of the interaction parameter, χ. Zhong and Masuoka[1] applied a cubic equation of state (i.e., Peng−Robinson EOS) to calculate gas solubilities in molten polymers in terms of temperature and pressure. Gauter et al.[8] used the Sanchez−Lacombe equation of state (SL EOS) to predict the cloud point isotherms of ethylene and *n*-hexane in PE. Koak et al.[9] studied the high-pressure behavior of ethylene/polyethylene and 1-butene/polybutene. The phase behavior of the two systems was modeled using the statistical associating fluid theory (SAFT) and the SL EOS. Orbey et al.[10] employed the SL EOS to calculate the phase equilibrium of a binary ethylene/polyethylene mixture in a low density PE process. They showed that the SL EOS could predict the ethylene/polyethylene phase equilibrium using only a single binary interaction parameter. In a series of publications by Sato et al.,[11−15] the solubilities of propylene in semicrystaline polypropylene, hexane in isotactic polypropylene, and CO_2 and N_2 in high density polyethylene (HDPE) and polystyrene were experimentally measured. The swelling behavior of the polymer caused by the sorbed species was calculated as a function of gas pressure and temperature using the SL EOS. Recently, Kiparissides et al.[2] measured the solubility of ethylene in

* To whom correspondence should be addressed. Tel.: + 30 2310 99 6211. Fax: +30 2310 996 198. E-mail: cypress@alexandros.cperi.certh.gr.

10.1021/ie060137j CCC: $33.50
Published on Web 07/19/2006

semicrystalline PE at elevated pressures and temperatures using a magnetic suspension microbalance. The experimentally measured solubilities were in excellent agreement with the corresponding values predicted by the SL EOS.

In general, the predictive capabilities of an EOS model strongly depend on a number of parameters that need to be determined experimentally. In fact, to predict the solubility of an olefin in an amorphous polymer, using the SL EOS, the characteristic parameters (i.e., P^*, T^*, and ρ^*) of both gaseous penetrant molecules and polymer need to be known. In addition, the value of a binary interaction parameter, k_{ij}, accounting for the interaction energy between the polymer segments and the sorbed molecules, should be known a priori. The estimation of the parameters appearing in an EOS model is usually carried out by fitting the selected EOS model to a series of experimental PVT and phase equilibrium data of the pure components as well as of their mixtures using nonlinear parameter estimation methods. To avoid the above tedious and costly experimental procedure, a molecular dynamics approach can be employed to calculate the characteristic parameters (e.g., P^*, T^*, and ρ^*) appearing in the SL EOS.

In the present study, the characteristic parameters (P^*, T^*, and ρ^*) were estimated using a molecular dynamics approach. Concurrently, experimental data on the solubilities of α-olefins in different types of polyolefins were utilized to estimate a single only parameter (i.e., the binary interaction parameter, k_{ij}) so that the SL EOS model predictions were in agreement with experimental solubility measurements over a wide range of temperatures, pressures, and polymer crystallinities.

Sanchez−Lacombe Equation of State

Since it is very difficult from an experimental point of view to measure experimentally the solubilities of all sorbed species of interest in different types of polymers, thermodynamic models, in the form of an EOS, are often employed to predict the phase behavior of a binary/ternary system. The SL EOS is one of the simplest statistical mechanics models that is capable of describing the phase behavior of an α-olefin/polyolefin binary system. Following the original developments of Sanchez and Lacombe,[16,17] the general EOS can be written as

$$\bar{\rho}^2 + \bar{P} + \bar{T}[\ln(1-\bar{\rho}) + (1 - 1/f)\bar{\rho}] = 0 \tag{1}$$

where $\bar{P} = (P/P^*)$, $\bar{\rho} = (\rho/\rho^*)$, and $\bar{T} = (T/T^*)$ are the respective reduced pressure, density, and temperature of a pure component. T, P, and ρ are the absolute temperature (K), pressure (bar), and the density (kg/m^3), while T^*, P^*, and ρ^* are some characteristic parameters of the pure component, respectively.

For a polymer chain, the number of sites (mers) occupied in the lattice, f, can be related to its molecular weight, M, according to the following equation:

$$f = P^*M/(RT^*\rho^*) \tag{2}$$

Note that for a high molecular weight polymer the value of f can be considered to be infinite. Accordingly, the characteristic parameters, P^*, T^*, and ρ^*, for a polymer chain are defined as follows:

$$T^* = \epsilon^*/R, \quad P^* = \epsilon^*/\nu^*, \quad \rho^* = M/(f\nu^*) \tag{3}$$

where ϵ^* is the mer−mer interaction energy, ν^* is the closed-packed molar volume of a mer, f is the number of mers a molecule occupies in the lattice, and R is the universal gas constant. For a pure substance, the values of the parameters P^*, T^*, and ρ^*can be determined by fitting the SL EOS to known experimental PVT data.

For a polymer−vapor mixture, it is necessary to use a mixing rule for the calculation of ϵ^*_{mix}, ν^*_{mix}, and f_{mix} based on the respective values of the pure components. Thus, by using the van der Waals-1 mixing rule, the characteristic close-packed molar volume of a mer of the mixture, ν^*_{mix}, can be defined as follows:

$$\nu^*_{mix} = \sum_{i=1}^{N_c}\sum_{j=1}^{N_c}\phi_i\phi_j\nu^*_{ij} \tag{4}$$

where,

$$\nu^*_{ij} = \frac{\nu^*_{ii} + \nu^*_{jj}}{2}(1 - n_{ij}) \tag{5}$$

The parameter n_{ij} accounts for possible deviations of ν^*_{ij} from the arithmetic mean value of the corresponding ν^*_{ii} and ν^*_{jj} values of the pure components. Accordingly, the values of ϵ^*_{mix} and f_{mix} of the mixture will be given by the following equations:

$$\epsilon^*_{mix} = \frac{1}{\nu^*_{mix}}\sum_{i=1}^{N_c}\sum_{j=1}^{N_c}\phi_i\phi_j((\epsilon^*_{ii}\,\epsilon^*_{jj})^{0.5}(1 - k_{ij}))\nu^*_{ij} \tag{6}$$

$$f_{mix}^{-1} = \sum_{j=1}^{N_c}(\phi_j/f_j) \tag{7}$$

where k_{ij} is a binary parameter, accounting for the interaction energy between the "i" and "j" species (mers) in the mixture. Similarly, the volume fraction of the i component in the mixture, ϕ_i, can be expressed in terms of the mass fraction ω_i and the characteristic values of ν^*_i and ρ^*_i of the pure components.

$$\phi_i = \frac{\omega_i}{\rho_i\nu_i}\left(\sum_{j=1}^{N_c}\left(\frac{\omega_j}{\rho^*_j\nu^*_j}\right)\right) \tag{8}$$

Following the developments of McHugh and Krukonis,[18] the chemical potential of the i component in a multicomponent system can be expressed as

$$\mu_i = RT\left[\ln\phi_i + \left(1 - \frac{f_i}{f_{mix}}\right)\right] + f_i\left(-\bar{\rho}\left[\frac{2}{\nu^*}\left(\sum_{j=1}^{N_c}\phi_j\nu^*_{ij}\epsilon^*_{ij} - \epsilon^*_{mix}\sum_{j=1}^{N_c}\phi_j\nu^*_{ij}\right) + \epsilon^*_{mix}\right]\right) + f_i\left(RT\bar{\nu}\left[(1-\bar{\rho})\ln(1-\bar{\rho}) + \frac{\bar{\rho}}{f_i}\ln\bar{\rho}\right] + P\bar{\nu}\left(2\sum_{j=1}^{N_c}\phi_j\nu^*_{ij} - \nu_{mix}\right)\right) \tag{9}$$

where N_c denotes the number of components in the mixture. At equilibrium, the chemical potentials of each component (i.e., 1 for penetrant and 2 for polymer) in a two-phase binary system will be equal:

$$\mu_i^{polymer} = \mu_i^{gas}, \quad i = 1, 2 \tag{10}$$

Thus, for given values of temperature and pressure, the volume fraction of the sorbed species in the polymer phase, φ_1, can be calculated by solving eq 10, using a nonlinear algebraic equation solver. In the present analysis, the value of the interaction parameter n_{ij} was assumed to be equal to zero.

The mass fraction of sorbed species in the amorphous polymer phase, ω_1, was calculated using eq 8. Finally, the corresponding equilibrium concentration of sorbed species in the amorphous polymer was calculated by eq 11.

$$[M]^* = S^*\rho_{am}/M = (\omega_1/\omega_2)\rho_{am}/M \quad (11)$$

where S^* (kg/(kg atm)) is the solubility coefficient of the sorbed species.

Provided that the characteristic parameters (T^*, P^*, and ρ^*) of the pure components (i.e., gas/vapor and polymer) as well as the value of k_{ij} are known, the SL EOS can be employed to predict the solubility of a penetrant gas in a polymer matrix under different temperatures and pressures.

Estimation of the T^*, P^*, and ρ^* Parameters

The estimation of the characteristic parameters, appearing in an EOS model, is a problem of profound importance for the thermodynamic analysis of chemical processes. There are several methods available in the literature that can be used to estimate the characteristic parameters in an EOS model. Usually, the values of the parameters of a pure component are obtained by fitting the model to available experimental PVT data. In this study, a molecular dynamics (MD) approach was employed to calculate the characteristic parameters (i.e., P^*, T^*, and ρ^*)[19] in the SL EOS.

Force field-based molecular simulation methods can in principle be used to make quantitative predictions of a range of thermodynamic properties in a binary system. When property predictions of comparable accuracy to experimental measurement are sought, considerable attention must be paid to crafting a force field which faithfully represents almost all energetic aspects of molecular behavior, including factors such as descriptions of the energy associated with distortions of bonds and angles, energies of different molecular conformers, and precise treatment of interactions between atoms in different molecules (or remotely located within the same molecule).[20] A number of force fields of varying degrees of complexity have been proposed.

In the present study, the COMPASS (condensed-phase optimized molecular potentials for atomistic simulation studies) force field was employed to estimate the pure component characteristic parameters (P^*, T^*, and ρ^*) appearing in the SL EOS.[20−22] COMPASS is an ab initio force field that has been parametrized and validated using condensed-phase properties in addition to various ab initio and empirical data for molecule isolation. The functional energy of the employed force field is given by the following expression:[21]

$$E_{total} = E_b + E_\theta + E_\phi + E_x + E_{bb'} + E_{b\theta} + E_{b\phi} + E_{\theta\theta'} + E_{\theta\theta'\phi} + E_{elec} + E_{ij} \quad (12)$$

The terms in the above equation can be divided into two categories: valence terms including diagonal and off-diagonal cross couplings and nonbonded interaction terms. The valence terms include E_b, E_θ, E_ϕ, and E_x for bond, angle, torsion, and out-of-plane angle coordinates, respectively. Moreover, the terms $E_{bb'}$, $E_{b\theta}$, $E_{b\phi}$, $E_{\theta\theta'}$, and $E_{\theta\theta'\phi}$ represent the cross-coupling terms between internal coordinates. The cross-coupling terms are important for predicting vibrational frequencies and structural variations associated with conformational changes. Among the cross-coupling terms, the bond−bond, $E_{bb'}$, bond−angle, $E_{b\theta}$, and bond−torsion, $E_{b\phi}$, terms are the most significant. The nonbonded term, which includes a "soft" Lennard−Jones 9-6 potential for the van der Waals interaction and a Coulombic contribution for electrostatic interactions, accounts for the interactions between pairs of atoms that are separated by three or more intervening atoms or those that belong to different molecules. The LJ parameters (ϵ and r^0) for like atom pairs are contained in the parametrization set. For unlike atom pairs, a 6th order combination law was used to calculate the parameters as follows:

$$\epsilon_{ij} = 2\sqrt{\epsilon_{ii}\epsilon_{jj}}\left[\frac{(r_{ii}^0 r_{jj}^0)^3}{(r_{ii}^0)^6 + (r_{jj}^0)^6}\right]; \quad r_{ij}^0 = \left[\frac{1}{2}((r_{ii}^0)^6 + (r_{jj}^0)^6)\right]^{1/6} \quad (13)$$

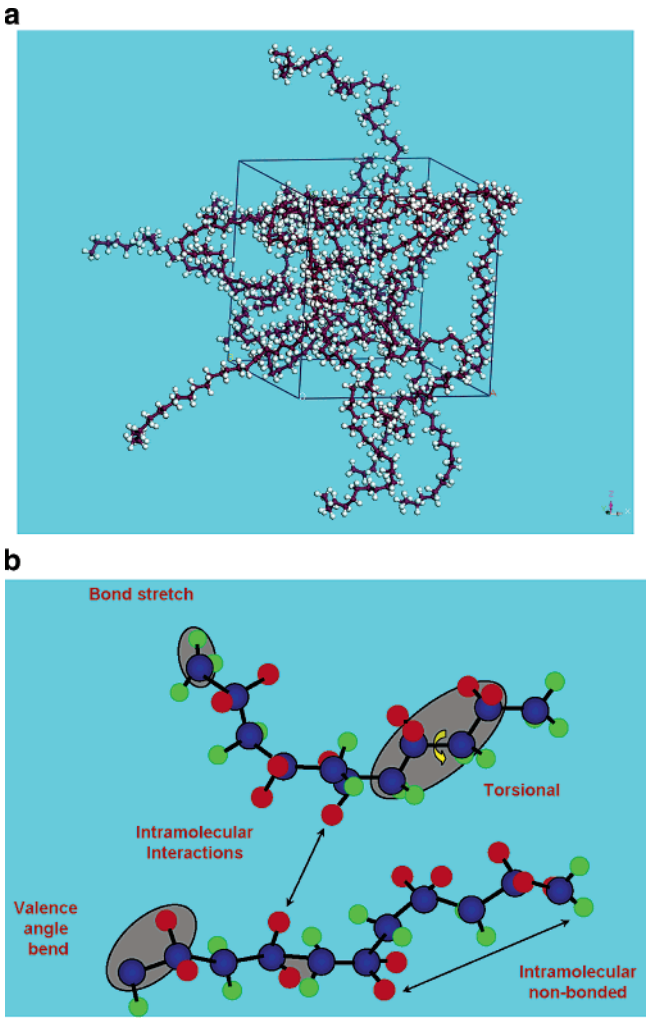

Figure 1. (a) Schematic representation of the simulation box. (b) Schematic representation of the force field used to carry out the MD simulations.

Molecular Dynamics Simulations. In the present study, the commercial software Materials Studio by Accelrys was used to carry out the molecular dynamics procedure. For every selected species (i.e., penetrant molecules and polymer chain), its molecular architecture was first built and its geometry was optimized by minimizing the energy of the system using the COMPASS force field.[20−22] The force field was represented by the internal coordinates of bond, angle, and torsion angle, and the cross-coupling terms included combinations of two or three internal coordinates (see Figure 1b).[22] Furthermore, one polymer long chain was constructed instead of many shorter polymer chains to avoid unusual free volume distributions as a result of the many polymer chain ends.[23] In addition, to minimize the discrepancies in the final characteristic density values obtained

Table 1. Pure Component Characteristic Parameters Calculated via the Molecular Dynamics Method

penetrants	T^* (K)	P^* (bar)	ρ^* (kg/m^3)
ethylene	283	3395	0.680
1-butene	410	3350	0.770
1-hexene	450	3252	0.814
1-octene	487	3300	0.842
propylene	346	3790	0.755
nitrogen	160	1038	0.81

polymers	T^*(K)	P^* (bar)	ρ^*(kg/m^3)
HDPE	650	4250	0.905
polypropylene	692	3007	0.890
impact polypropylene	689	3175	0.890
LLDPE-1-Butene	667	4370	0.900
LLDPE-1-Hexene	653	4360	0.903
LLDPE-1-Octene	660	4140	0.906

from the MD technique, the initial polymer chain density was assumed to be equal to the corresponding available literature values.[23,24] Accordingly, the polymer structures were relaxed to the minimum energy, while random atom overlaps were avoided by using the conjugate-gradient method.[25] To prevent the system's entrapment in a local high-energy minimum, the relaxed polymer structures were subjected to simulated annealing (e.g., five repeated cycles from 400 to 1000 K and back) by using a constant number of moles, constant volume, and constant temperature (i.e., NVT) molecular dynamic conditions. It should be pointed out that, at the end of each annealing cycle, the polymer structures were again relaxed and the simulation "box" was allowed to vary in size during energy minimization in order to achieve the equilibrium density for each polymer structure. Notice that each simulation was running for 10^6 molecular dynamic steps of 1 fs (i.e., 1 ns of total time).

On the basis of the fully relaxed models of the corresponding polymeric chains, isothermal−isobaric (i.e., NPT) molecular dynamic experiments were run at 373 K (i.e., a temperature above the glass transition temperature of the polymers of interest) and from 350 to 50 K at equal temperature intervals of 50 K. It is noted that the calculation of the equation of state characteristic parameters at 0 K was made by extrapolation. Specifically, the simulation results (i.e., 5×10^6 molecular dynamic steps) obtained from five different relaxed structures of the polymer chain, according to the procedure described above, were employed to calculate the characteristic parameters of the SL EOS.

The kinetic energy value, obtained from the molecular dynamics procedure, extrapolated at 0 K was practically equal to 0 which is quite sensible since any thermal motion vanishes at 0 K (i.e., a structure with the lower total energy). Under these conditions, the characteristic density is obtained from the simulation box size at 0 K and the potential energy, E_{pot}, was equal to the total energy, E_{tot}. Thus, the characteristic pressure directly corresponded to the cohesive energy density at 0 K, e_{coh}^0. In general, e_{coh} is defined as the ratio between the cohesive energy E_{coh} and the molar volume at a given temperature. E_{coh} is defined as the increase in internal energy per mole of substance, assuming that the intermolecular forces are negligible. Due to fact that each polymer chain is surrounded by other chains that are simply displaced images of the chain itself, the cohesive energy is associated with the energy of the interactions between these images. Accordingly, the values of E_{coh} at different temperatures were obtained from simulation runs by calculating the difference between the nonbonded energy of the periodic polymer structure, $E_{nb}^{periodic}$, and the corresponding value for an isolated parent polymer chain in a vacuum, $E_{nb}^{isolated}$. The cohesive energy at 0 K was calculated by extrapolation. Finally, the T^* parameter was obtained by substituting the corresponding P^*, ρ^*, P, and ρ values at the highest simulated temperature into eq 1. In Table 1, the calculated values of the characteristic parameters T^*, P^*, and ρ^* are shown for various gas/vapor olefin−polyolefin binary systems.

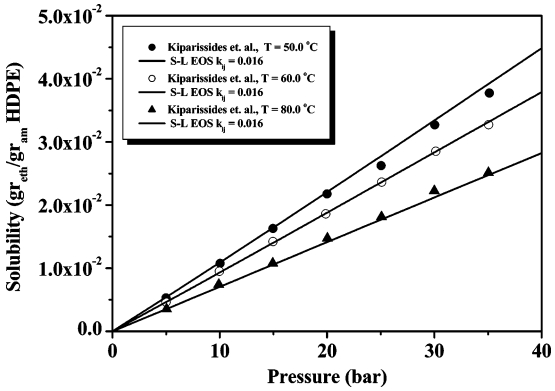

Figure 2. Solubility of ethylene in HDPE at different temperatures, ω_c = 73.8%.

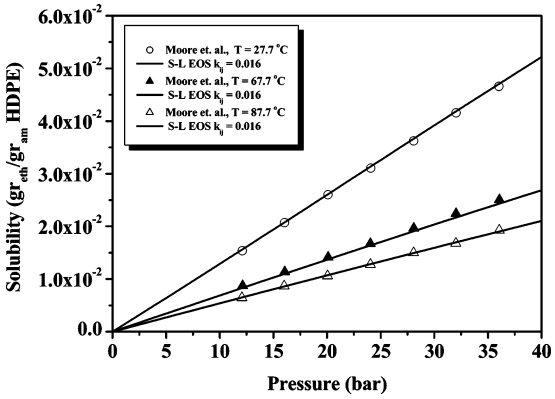

Figure 3. Solubility of ethylene in HDPE at different temperatures, ω_c = 73.3%.

Results and Discussion

Solubility of Ethylene in HDPE and LLDPE. In Figures 2 and 3, the experimentally measured ethylene solubilities in HDPE[2,26] at different pressures and temperatures are compared with model predictions obtained by the SL EOS. It is important to point out that in all theoretical calculations the values of the T^*, P^*, and ρ^* parameters were directly obtained from the MD simulations (see Table 1) while the value of the interaction parameter, k_{ij}, was kept constant (i.e., $k_{ij} = 0.016$) for all tested temperatures. Note that, in all cases, the polymer crystallinity was approximately equal to 74% w/w, which explains the constant value of k_{ij} at all tested temperatures.

In Figures 4 and 5, experimental and predicted solubilities of ethylene in linear low density ethylene-1-Butene and ethylene-1-Hexene copolymer grades are plotted. As can be seen, the theoretical predictions are in excellent agreement with the available experimental data. However, it should be pointed out that, contrary to the ethylene/HDPE binary system, the value of the interaction parameter for the ethylene/LLDPE binary systems strongly depends on the temperature, due to the presence of the comonomer in the copolymer chains. The variation of the interaction parameter, k_{ij}, with respect to temperature for these systems is depicted in Figure 6. As can been seen, the binary interaction parameter for both systems exhibits the same

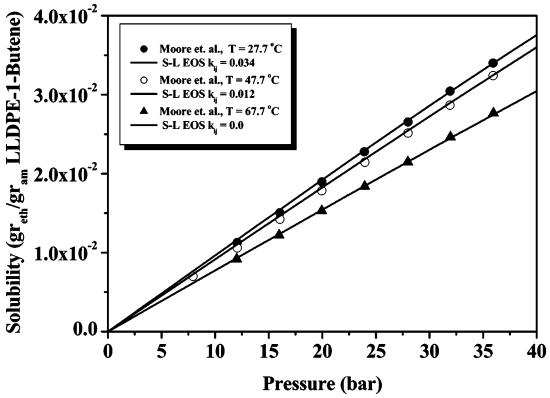

Figure 4. Solubility of ethylene in LLDPE-1-Butene at different temperatures.

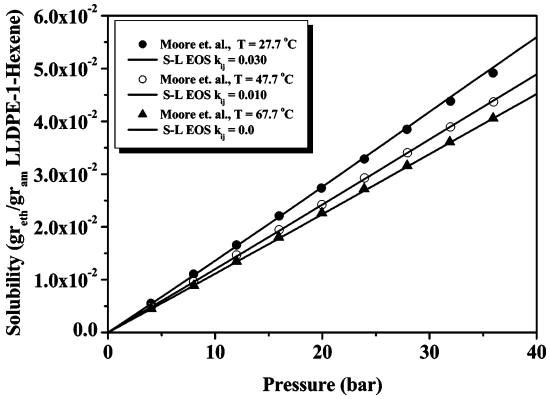

Figure 5. Solubility of ethylene in LLDPE-1-Hexene at different temperatures.

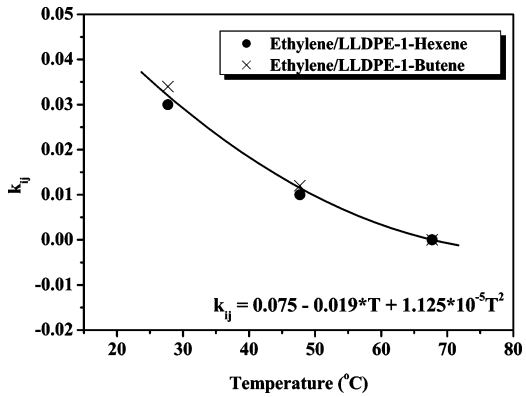

Figure 6. Variation of the interaction parameter, k_{ij}, with respect to temperature in ethylene/LLDPE binary systems.

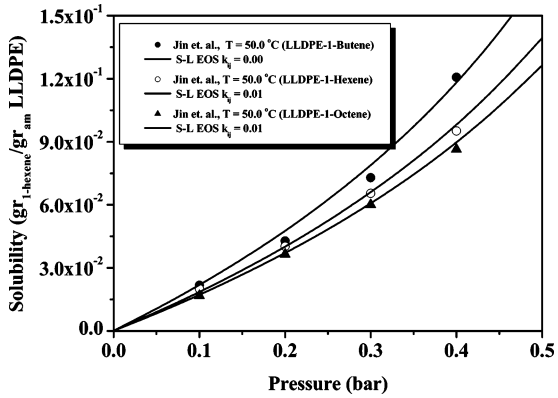

Figure 7. Solubility of 1-hexene in LLDPE-1-Butene, LLDPE-1-Hexene, and LLDPE-1-Octene at $T = 50$ °C.

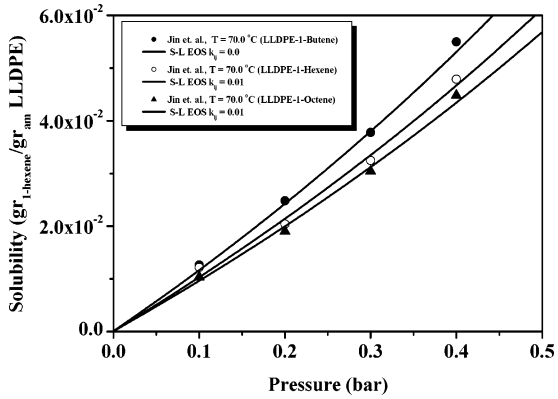

Figure 8. Solubility of 1-hexene in LLDPE-1-Butene, LLDPE−1-Hexene, and LLDPE-1-Octene at $T = 70$ °C.

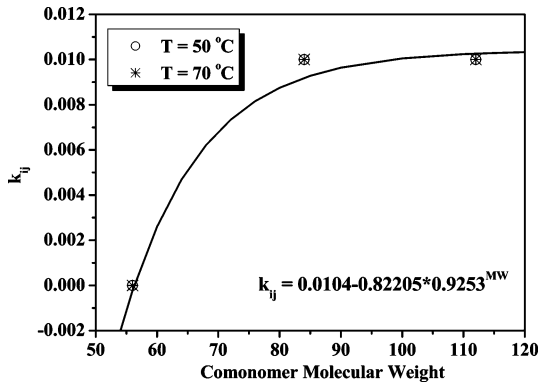

Figure 9. Variation of the interaction parameter, k_{ij}, with respect to comonomer molecular weight and temperature in 1-hexene/LLDPE binary systems.

exponential decrease with temperature. In fact, at higher temperatures (e.g., $T > 65$ °C), the k_{ij} asymptotically approaches zero (i.e., the interactions between the polymer segments and the penetrant molecules are negligible).

Solubility of 1-Hexene in LLDPE. The experimental measurements of Jin et al.[27] on the solubility of 1-hexene in various LLDPEs (i.e., ethylene-1-Hexene, ethylene-1-Butene, and ethylene-1-Octene copolymers) were also used to verify the predictive capabilities of the SL EOS. In Figures 7 and 8, the experimental and theoretical solubilities of 1-hexene in different types of LLDPE are depicted at 50 and 70 °C, respectively. Note that in all theoretical calculations the values of the T^*, P^*, and ρ^* parameters for the sorbed species and the copolymers were directly obtained from the MD simulations. It is evident that the solubility of 1-hexene in the various LLDPE grades depends both on the comonomer type and temperature. In fact, as the temperature increases, the solubility of 1-hexene in LLDPE decreases (see Figures 7 and 8). On the other hand, as the molecular size of the comonomer decreases, the solubility of 1-hexene in LLDPE increases. It is important to point out that the value of the binary interaction parameter, k_{ij}, for the 1-hexene in all tested LLDPEs is independent of temperature. On the other hand, the binary interaction parameter increases from a value of $k_{ij} = 0$ to a final value of $k_{ij} = 0.01$ as the molecular weight of the comonomer in the copolymer increases (see Figure 9).

In Figures 10−12, the experimentally measured 1-hexene solubilities in linear low-density ethylene-1-Hexene copolymer (LLDPE-1-Hexene),[27] at different pressures, temperatures, and polymer crystallinities, are compared with model predictions obtained by the SL EOS. As can be seen, the theoretical predictions are in excellent agreement with the available

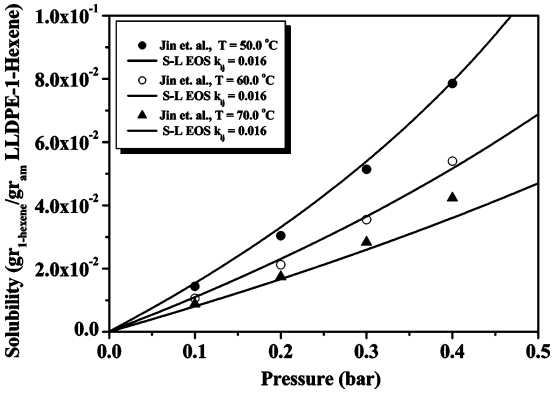

Figure 10. Solubility of 1-hexene in LLDPE-1-Hexene at different temperatures, $\omega_c = 40.7\%$.

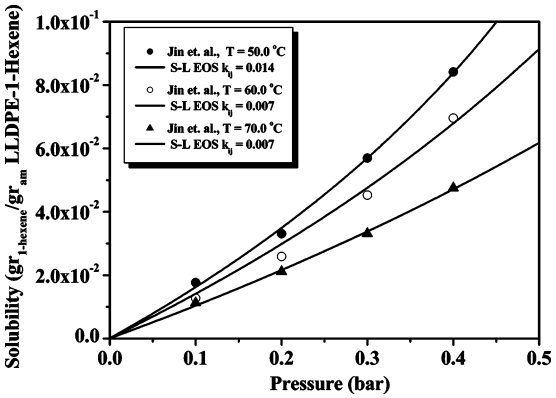

Figure 11. Solubility of 1-hexene in LLDPE-1-Hexene at different temperatures, $\omega_c = 26.0\%$.

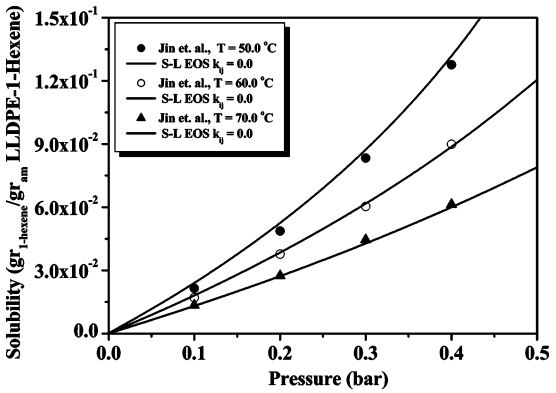

Figure 12. Solubility of 1-hexene in LLDPE-1-Hexene at different temperatures, $\omega_c = 0.0\%$.

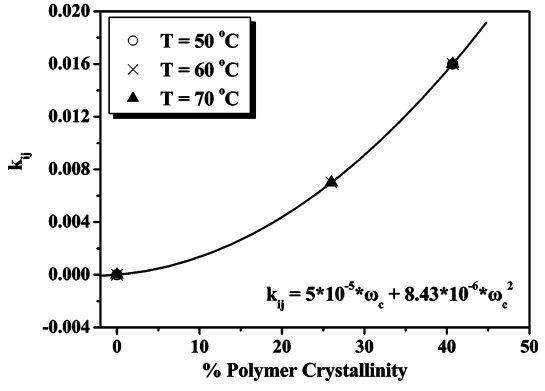

Figure 13. Variation of the interaction parameter, k_{ij}, with respect to polymer crystallinity and temperature in the 1-hexene/LLDPE-1-Hexene binary system.

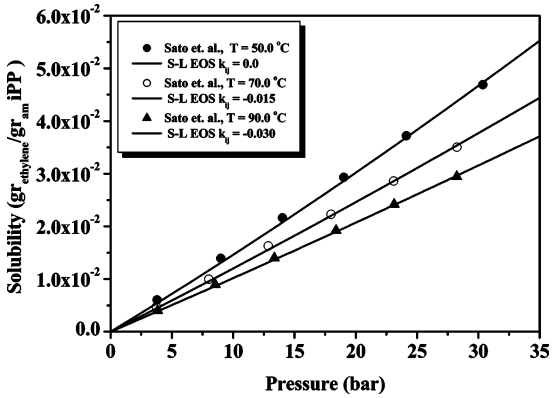

Figure 14. Solubility of ethylene in iPP.

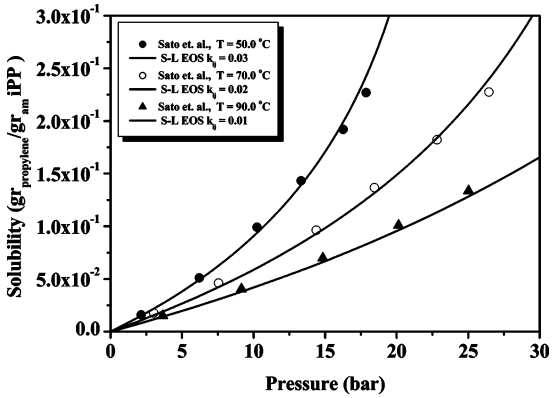

Figure 15. Solubility of propylene in iPP.

experimental data. Notice that, in all cases, the α-olefin solubility decreases as the temperature increases. It should be pointed out that the value of the interaction parameter for the 1-hexene/LLDPE-1-Hexene binary system strongly depends on the polymer crystallinity (see Figure 13). In fact, at high polymer crystallinities, the interaction between the polymer segments and the penetrant molecules increases. On the other hand, in the sorption of 1-hexene in a fully amorphous LLDPE-1-Hexene copolymer (i.e., $\omega_c = 0.0$), the value of k_{ij} asymptotically approaches zero, independently of temperature.

Solubility of Ethylene and Propylene in Polypropylene and Impact Polypropylene. The experimental measurements of Sato et al.[14] on the solubilities of various α-olefins (i.e., ethylene and propylene) in impact polypropylene (iPP) were used to verify the predictive capabilities of the SL EOS. In Figures 14 and 15, the experimental and theoretical solubilities of ethylene and propylene in iPP are illustrated at different pressures and temperatures. As can be seen, the solubility of ethylene in iPP varies almost linearly with respect to pressure at all tested temperatures. However, contrary to the ethylene/iPP binary system, the solubility of propylene in iPP exhibits a strongly nonlinear behavior as the pressure increases. Moreover, as the molecular size of the penetrant increases, the value of the interaction parameter increases. This means that, for higher α-olefins at a certain temperature, the interaction activity between the unlike molecules (i.e., polymer segments and penetrant molecules) increases.

In Figures 16 and 17, the experimental and theoretical solubilities of propylene in PP are shown at different temperatures, pressures, and polymer crystallinities. It should be pointed out that, at low pressures (e.g., $P < 15$ bar) and low polymer crystallinities (e.g., $\omega_c = 19\%$), the interaction parameter of the propylene/PP binary system is almost independent of temperature (see Figure 16). On the other hand, at high pressures

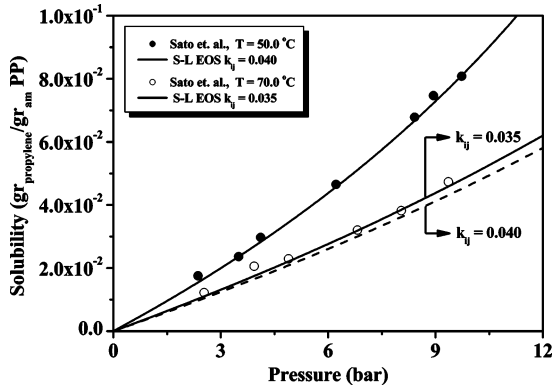

Figure 16. Solubility of propylene in PP at different temperatures, ω_c = 19.0%.

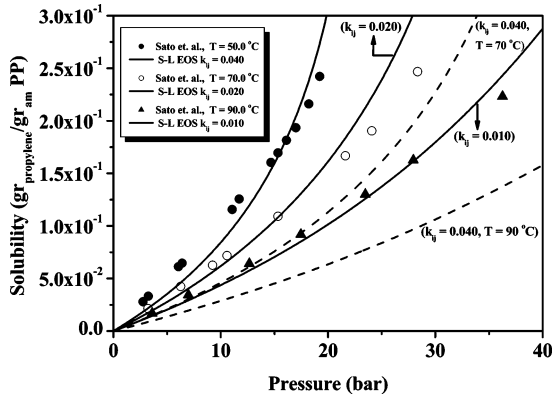

Figure 17. Solubility of propylene in PP at different temperatures, ω_c = 68.9%.

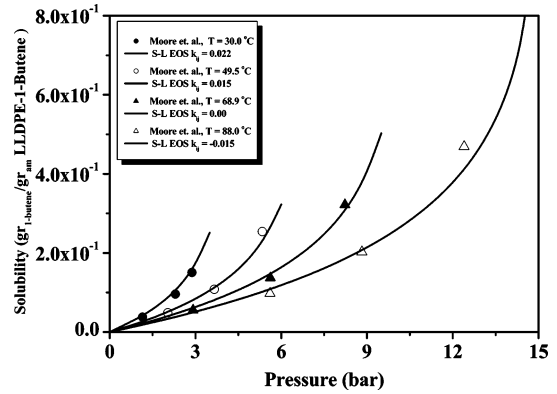

Figure 18. Solubility of 1-butene in LLDPE-1-Butene at different temperatures.

and polymer crystallinities (e.g., ω_c = 68.9%), the k_{ij} exhibits a strong dependence on temperature, and thus, a single value for k_{ij} cannot be applied (see the broken lines in Figure 17).

Solubility of 1-Butene in HDPE and LLDPE. The experimental measurements of Moore et al.[26] on the solubility of 1-butene in HDPE and various LLDPEs (i.e., ethylene-1-Butene and ethylene-1-Hexene copolymers) were compared with model predictions obtained by the SL EOS. In Figures 18−20, the experimental and theoretical solubilities of 1-butene in different types of PE are depicted over a wide range of temperatures and pressures. It is apparent that the theoretical predictions are in excellent agreement with the available experimental data. Notice that, in this case, the 1-butene solubility in various LLDPEs will depend on several factors including temperature, polymer crystallinity, and comonomer type. It is shown that as the comonomer size increases the solubility increases, independently of temperature. It is also important to point out that the values

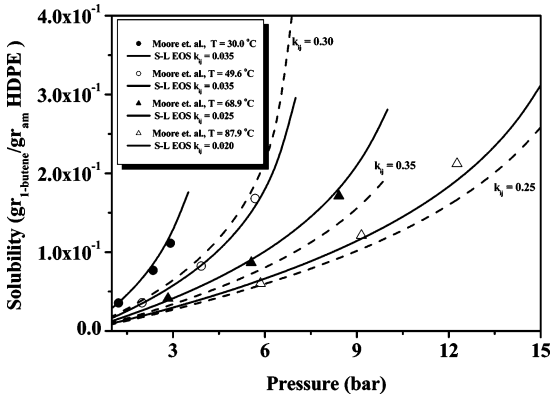

Figure 19. Solubility of 1-butene in HDPE at different temperatures.

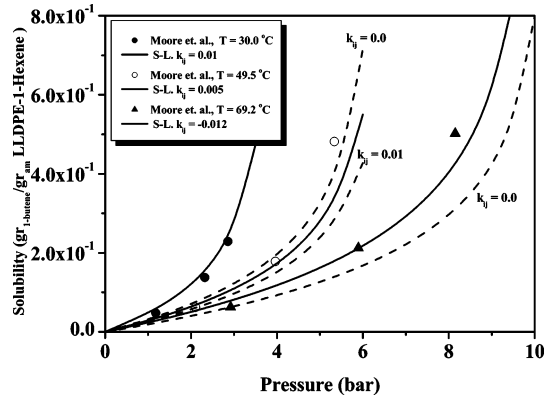

Figure 20. Solubility of 1-butene in LLDPE-1-Hexene at different temperatures.

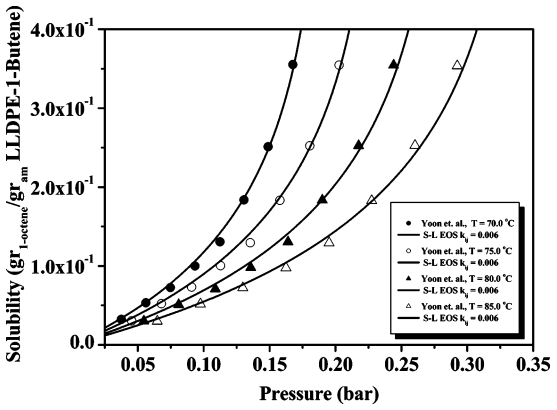

Figure 21. Solubility of 1-octene in LLDPE-1-Butene at different temperatures.

of the k_{ij} parameter for the 1-butene/LLDPE binary system decrease with respect to the comonomer type in the copolymer chains for all tested temperatures. Finally, in Figures 19 and 20, the effect of the k_{ij} parameter on the SL EOS predicted solubilities of 1-butene in HDPE and LLDPE-1-Hexene copolymer are illustrated, at various temperatures. As can be seen, the theoretically obtained solubilities are very sensitive to the selected values of the interaction parameter (e.g., see the broken lines in Figures 19 and 20) due to the nonlinear solubility behavior of 1-butene with respect to pressure. This can lead to significant deviations between the predicted and experimentally measured solubilities, especially, at high pressures.

Solubility of 1-Octene in LLDPE. In Figure 21, the predicted and experimentally measured solubilities of 1-octene in LLDPE-1-Butene are plotted.[28] It is important to point out that, in all theoretical calculations, the values of the T^*, P^*, and ρ^* parameters were directly obtained from the MD simulations (see

Table 1) while the value of the interaction parameter, k_{ij}, was kept constant (i.e., $k_{ij} = 0.006$) due to the low variation of pressure.

Conclusions

In the present study, it was shown that the SL EOS can be applied to predict the solubility of α-olefins in polyolefins over a wide range of pressures, temperatures, copolymer grades, and polymer crystallinities. For the theoretical prediction of solubilities, the values of the characteristic parameters of the pure components (i.e., P^*, T^*, and ρ^*), appearing in the SL EOS, were obtained via MD simulations. It was found that the MD method provided good estimates of the P^*, T^*, and ρ^* characteristic parameters. Thus, the only unknown parameter in the SL EOS was the value of binary interaction parameter k_{ij}. The value of k_{ij} was estimated for different binary α-olefins/polyolefins systems by fitting model predictions to experimentally measured solubilities.

Acknowledgment

The authors gratefully acknowledge the European Community for supporting this work under the Growth Projects G5RD-CT-2001-00597 and G5RD-CT-2002-00720.

Nomenclature

E_{total} = total energy, J/mol
E_{coh} = cohesive energy of the system, J/mol
e_{coh}^0 = cohesive energy density at 0 K, J
$E_{nb}^{isolated}$ = isolated nonbonded energy polymer chain in a vacuum, J
$E_{nb}^{periodic}$ = nonbonded energy of the periodic polymer stress, J
E_{pot} = potential energy of the system, J
f = pure component parameter
f_{mix} = mixture parameter
k_{ij} = interaction parameter
M = molecular weight of the pure component, kg/kmol
$[M]^*$ = penetrant concentration in the amorphous polymer, kg/m^3
N_c = number of components in the mixture
n_{ij} = interaction parameter
P = penetrant pressure, atm
$\bar{P}$ = reduced pressure
P^* = characteristic parameter, atm
r_{ij} = distance between Lennard−Jones species, Å
R = universal gas constant, J/(K mol)
S^* = equilibrium solubility coefficient, kg/(kg atm)
T = absolute temperature, K
$\bar{T}$ = reduced temperature
T^* = characteristic parameter, K
ν^*= close-packed molar volume of a mer, m^3/mol
ν_{mix}^* = close-packed molar volume of a mer of the mixture, m^3/mol

Greek Letters

ϵ^* = mer−mer interaction energy, J/mol
ϵ_{mix}^* = interaction energy of the mixture, J/mol
ϵ_{ij} = potential energy, J/mol
μ_i = chemical potential of the i component in the mixture
$\mu_i^{polymer}$ = chemical potential of a component in the polymer phase
μ_i^{gas} = chemical potential of a component in the gas phase
ρ = absolute density, kg/m^3
$\bar{\rho}$ = reduced density
ρ^* = characteristic close-packed mass density, kg/m^3
ρ_{am} = density of the amorphous phase, kg/m^3
ϕ_i = volume fraction of the i component in the mixture
ω_i = mass fraction of the of the i component in the mixture
ω_c = degree of polymer crystallinity

Literature Cited

(1) Zhong, C.; Masuoka, H. Modeling of Gas Solubilities in Polymers with Cubic Equation of State. *Fluid Phase Equilib.* **1998**, *144*, 49.

(2) Kiparissides, C.; Dimos, V.; Boultouka, T.; Anastasiades, A.; Chasiotis, A. Experimental and Theoretical Investigation of Solubility and Diffusion of Ethylene in Semicrystalline PE at Elevated Pressures and Temperatures. *J. Appl. Polym. Sci.* **2003**, *87*, 953.

(3) Hernadez-Munoz, P.; Gavara, R.; Hernadez, R. J. Evaluation of Solubility and Diffusion Coefficients in Polymer Film-Vapor Systems by Sorption Experiments. *J. Membr. Sci.* **1999**, *154*, 195.

(4) Chen, C. M. Gas Phase Olefin Copolymerization with Ziegler-Natta Catalysts. Ph.D. Thesis, University of Wisconsin−Madison, Madison, Wisconsin, 1991.

(5) Sarti, G. C., Doghieri, F. Predictions of the Solubility of Gases in Glussy Polymers Based on the NELF Model. *Chem. Eng. Sci.* **1998**, *53*, 3435.

(6) Doghieri, F.; Sarti, G. C. Predicting the Low Pressure Solubility of Gases and Vapors in Glussy Polymers by the NELF Model. *J. Membr. Sci.* **1998**, *147*, 73.

(7) Yoon, J. S.; Yoo, h. S.; Kang, K. S. Solubility of α-Olefins in Linear Low Density Polyethylenes. *Eur. Polym. J.* **1996**, *32*, 1333.

(8) Gauter, K.; Heidemann, R. A. Modeling Polyethylene-Solvent Mixtures with the Sanchez-Lacombe Equation. *Fluid Phase Equilib.* **2001**, *183−184*, 87.

(9) Koak, N.; Visser, R. M.; de Loos, Th. W. High-Pressure Phase Behaviour of the Systems Polyethylene+Ethylene and Polybutene+1-Butene. *Fluid Phase Equilib.* **1999**, *158−160*, 835.

(10) Orbey, H.; Bokis, C. P.; Chen, C. C. Equation of State Modeling of Phase Equilibrium in the Low-Density Polyethylene Process: The Sanchez−Lacombe, Statistical Associating Fluid Theory, and Polymer-Soave−Redlich−Kwong Equations of State. *Ind. Eng. Chem. Res.* **1998**, *37*, 4481.

(11) Sato, Y.; Yurugi, M.; Fujiwara, K.; Takishima, S.; Masuoka, H. Solubilities of Carbon Dioxide and Nitrogen in Polystyrene Under High Temperature and Pressure. *Fluid Phase Equilib.* **1996**, *125*, 129.

(12) Sato, Y.; Fujiwara, K.; Takikawa, T.; Sumarno; Takishima, S.; Masuoka, H. Solubilities and Diffusion Coefficients of Carbon Dioxide and Nitrogen in Polypropylene, High-density Polyethylene and Polystyrene Under High Pressures and Temperatures. *Fluid Phase Equilib.* **1999**, *162*, 261.

(13) Sato, Y.; Tsuboi, A.; Sorakubo, A.; Takishima, S.; Masuoka, H.; Ishikawa, T. Vapor-Liquid Equilibrium Ratios for Hexane at Infinite Dilution in Ethylene+Impact Polypropylene Copolymer and Propylene+Impact Polypropylene Copolymer. *Fluid Phase Equilib.* **2000**, *170*, 49.

(14) Sato, Y.; Yurugi, M.; Yamabiki, T.; Takishima, S.; Masuoka, H. Solubility of Propylene in Semicrystalline Polypropylene. *J. Appl. Polym. Sci.* **2001**, *79*, 1134.

(15) Sato, Y.; Takikawa, T.; Takishima, S.; Masuoka, H. Solubilities and Diffusion Coefficients of Carbon Dioxide in Poly(vinyl acetate) and Polystyrene. *J. Supercrit. Fluids* **2001**, *19*, 187.

(16) Sanchez, I. C.; Lacombe, R. H. An Elementary Molecular Theory of Classical Fluids. Pure Fluids. *J. Phys. Chem.* **1976**, *80*, 2352.

(17) Sanchez, I. C.; Lacombe, R. H. Statistical Thermodynamics of Polymer Solutions. *Macromolecules* **1978**, *11*, 1145.

(18) McHugh, M.; Krukonis V. *Supercritical Fluid Extraction*, 2nd ed.; Butterworth-Heinemann Publishing: Woburn, MA, 1994.

(19) Fermeglia, M.; Pricl, S.; Equation-of-State Parameters for Pure Polymers by Molecular Dynamics Simulations. *AIChE J.* **1999**, *45*, 2619.

(20) Rigby, D. Fluid Density Predictions Using the COMPASS Force Field. *Fluid Phase Equilib.* **2004**, *217*, 77.

(21) Sun, H.; Ren, P.; Fried, J. R. The COMPASS Force Field: Parametrization and Validation for Phosphazenes. *Comput. Theor. Polym. Sci.* **1998**, *8*, 229.

(22) Sun, H. COMPASS: An ab Initio Force-Field Optimized for Condensed-Phase Applications-Overview with Details on Alkane and Benzene Compounds. *J. Phys. Chem.* **1998**, *102*, 7338.

(23) Jo, W. H.; Choi, K. Determination of Equation-of-State Parameters by Molecular Simulations and Application to the prediction of Surface Properties for Polyethylene. *Macromolecules* **1997**, *30*, 1800.

(24) Li, Y.; Mattice, W. L.; Atom Based Modeling of Amorphous 1,4-cis-Polybutadiene. *Macromolecules* **1992**, *25*, 4942.

(25) Fan, C. F.; Cagin, T.; Chen, Z. M.; Smith, K. A. Molecular Modeling of Polycarbonate. 1. Force Field Static Structure, and Mechanical Properties. *Macromolecules* **1994**, *27*, 2383.

(26) Moore, S. J.; Wanke, S. E. Solubility of Ethylene, 1-Butene and 1-Hexene in Polyethylenes. *Chem. Eng. Sci.* **2001**, *56*, 4121.

(27) Jin, H. J.; Kim, S.; Yoon, J. S. Solubility of 1-Hexene in LLDPE Synthesized by (2-Melnd)$_2$ZrCl$_2$/MAO and by Mg(OEt)$_2$/DIBP/TiCl$_4$-TEA. *J. Appl. Polym. Sci.* **2002**, *84*, 1566.

(28) Yoon, J. S.; Chung, C. Y.; Lee, L. H. Solubility and Diffusion Coefficient of Gaseous Ethylene and α-Olefin in Ethylene/α-Olefin Random Copolymer. *Eur. Polym. J.* **1994**, *30*, 1209.

Received for review February 2, 2006
Revised manuscript received May 8, 2006
Accepted May 22, 2006

IE060137J